



(REVIEW ARTICLE)



Interactions, space presentations, blocks and cross products

Gudrun Kalmbach HE *

MINT, PF 1533, D-86818 Bad Woerishofen, Germany.

GSC Advanced Research and Reviews, 2021, 06(02), 061-073

Publication history: Received on 04 January 2021; revised on 03 February 2021; accepted on 05 February 2021

Article DOI: <https://doi.org/10.30574/gscarr.2021.6.2.0012>

Abstract

Physics counts four basic forces, the electromagnetic EMI, weak WI, strong SI interactions and gravity GR. The first three are provided with a unified theory which partly needs revision and has the symmetry $U(1) \times SU(2) \times SU(3)$. In this article their space presentations are described in order to include a theory for gravity which cannot be added directly to the standard model. There are many instances of gravitational actions which are different from the other three interactions. Gravity uses geometrical models beside spacetime, often projective, including stereographic and spiralic orthogonal subspace projections. Real and complex cross products, symmetries which belong to the complex Moebius transformation subgroups, complex cross ratios, Gleason frame GF measures, dihedrals nth roots of unity with symmetries are some new tools (figure 14) for a new gravity model.

The basic vector space is 8-dimensional, but beside the usual vector addition and calculus there are different multiplications added. The author uses complex multiplications in the complex 4-dimensional space C^4 for calculus. The $SU(3)$ multiplication of GellMann 3×3 -matrices is used for C^3 and its three 4-dimensional C^2 projections. Projective spaces are CP^2 for nucleons and a GR Higgs plane P^2 and projective measuring GF's which have 3-dimensional, orthogonal base vectors like spin. The doubling of quaternionic spacetime to octonians has a different multiplication and seven GF's which partly occur in physics as cross product equations. Beside the real, the complex cross product extends the spacetime dimensions from 4 to 8. Consequences are that there are many 3-dimensional, many 4-dimensional, some 6-dimensional and also projective 5-dimensional spaces in which the actions of gravity can then be described. Spacetime is for this not sufficient. No symmetry can be multiplied to the standard model since the new symmetries belong to different geometries and are not directly related to a set of field quantum particles like one photon for EMI, three weak bosons (or four) for WI, eight gluons for SI. GR has graviton waves similar to EMI waves and in quasiparticle form rgb-graviton whirls, for mass Higgs bosons, maybe also solitons (density as mass per volume changing). They attribute to a distance metric between two points (kept fixed) an amplitude density (operator) which changes the metrical diameter of the volume, but not the mass.

Keywords: Cross product; Quantization; Interaction; Spaces; Octonians

1. Cross products

The real cross product for space coordinates x, y, z measures with the length of the vector on the z -axis the area of two nonzero vectors in the xy -plane. The quantized length scaling in meter is observed through the three spin coordinates. The quantization is due to the fact that winding numbers on a complex circle are counted in time t and frequency f is measured as an inverse time interval $f = 1/\Delta t$ or as angular frequency $\omega = d\varphi/dt = 2\pi f$, φ complex polar angle. In getting the $SU(2)$ symmetry for spacetime, the coordinates x, y, z are replaced by Euler angles which have 2×2 -matrices for presenting them as transformations. Their multiplication is like the Pauli spin matrices and they make these three noncommutative quaternionic $SU(2)$ generators. As group generators they first use the base change from $(1\ 0)$, $(0\ 1)$ in

* Corresponding author: Gudrun Kalmbach H.E
MINT, PF 1533, D-86818 Bad Woerishofen, Germany.

the xy-plane to (0 1), (-1 0) (a 90 degree rotation) and list in this order the columns of two transformation matrices σ_1 and σ_2 where the second matrix multiplies like the complex numbers in $x \cdot i + y \cdot \sigma_2$. The complex numbers for calculus are available, also as operators.

The real cross product exists in any dimension: for a real space R^n , the cross product $y^{(n+1)} = y_1 \times \dots \times y_n$ exists. For $n = 3$, a volume is measured. This belongs to heat T which measures an entropy inside a volume V and matter inside V generates on the surface of V a pressure p with $p \cdot V = b \cdot T$, b a real constant. The complex cross product uses two linear independent complex vectors which can be located in one complex z -plane. It exists also in any dimension. The coordinate $z = x + iy$ is not the real space coordinate z . It can also be used for extending a 2-dimensional C^2 to a 3-dimensional complex space C^3 . An Einstein mass-frequency plane $z_3 = (m, f) = z_1 \times z_2$ can be added to $(z_1 = z + ict, z_2 = x + iy)$ spacetime coordinates. This is necessary for gravity with mass, set at barycenters of matter. For nucleons mass a GF adds three masses of quarks as 10 percent of the nucleon mass, adds about 80 percent speeds/frequency mass through $mc^2 = hf$ in the (m, f) -plane and 10 percent similar energies from interactions. When nucleons barycentric coordinates are constructed, a Higgs boson can set at the nucleons barycenter the new GF measure for nucleons mass.

In Pauli 2x2-matrix form C^2 is presented having $(z_1 \ z_2)$ as first and $(-c(z_2) \ c(z_1))$ as second row where c means complex conjugation. The first Pauli matrix uses the base (0 1), (1 0) as first and second row, the third (1 0), (0 -1) in this order. This setting is extended to C^3 with (z_1, z_2, z_3) coordinates by using SU (3) GellMann 3x3-matrices. These matrices are projection maps, extended from the three Pauli matrices by inserting a row and column with coordinates 0. The three extended σ_3 matrices $\lambda_3, \lambda_9, \lambda_{10}$ are linearly dependent and for the indices 9,10 these matrices are scaled and added to one λ_8 coordinate for 8, not 9 gluons. The MINT Wigris model treats λ_8 later on for another use. The first coordinate projection 3x3-matrix has as rows $(z_1 \ z_2 \ 0)$ first, $(-c(z_2) \ c(z_1) \ 0)$ second and third (0 0 0), the second such matrix has $(z_1 \ 0 \ z_3)$ first, (0 0 0) second and $(-c(z_3) \ 0 \ c(z_1))$ third row, the third projection matrix has (0 0 0) first, (0 $z_2 \ z_3$) second and third (0 $-c(z_3) \ c(z_2)$).

There are three complex 2-dimensional spaces C^2 with coordinates (z_i, z_j) for $i, j = 1, 2$ or $2, 3$ or $1, 3$ generated for an electrical potential, weak interaction space 1234, numbered by octonian coordinate indices, 3456 for a gravity potential, strong interaction space and 1256 for an EMI space.

The complex spaces 1256, 3456 have projections into 1234 which makes empty spacetime to an energy or fields carrying system. It is useful to show their fiber bundle presentation with S^1 as fiber. 1234 has the Hopf fiber bundle [1] with space the unit sphere S^3 in R^4 and the map $h: S^3 \rightarrow S^2$, 3456 has the nucleon/atomic kernels fiber bundle with space the unit sphere S^5 in R^6 or C^3 and map $g: S^5 \rightarrow CP^2$, a complex projective 2-dimensional space with boundary S^2 . The twisted product $S^3 \times S^5$ space is the SU (3) geometry. The first factor is projected down to the WI S^3 Hopf sphere by rgb-gravitons which use the first three GellMann matrices with a third row and column 0.

CP^2 is observed as bubbles in spacetime for which the Pauli principle holds.

The EMI space has its rolled coordinate 7 as transversal circle (replacing 1) of a cylinder with common central axis for the z -coordinate and its time 4 generated world line, 6 is for the EMI frequency and 5 for its relativistic mass. Its wave presentation is observable as cosine function (projection) in spacetime and the cylinder axis as its linear world line. EMI is generated with photons as field quanta much later than nucleons in the early development of the universe. For them another complex coordinate has to be added as cross product $z_4 = z_1 \times z_2 \times z_3$. EMI and its U(1) circle symmetry is a e_7 octonian, rolled Kaluza-Klein coordinate $\exp(i\varphi)$, φ polar complex angle, for presenting wave functions through exp functions. The first coordinate of z_3 is an octonian vectorial coordinate e_0 . It provides on U (1) for n th roots of unity the n segments of the complex disk with U (1) as boundary. The discrete turning of e_0 is a spherical angle θ , measured towards the positive space z -axis. It is observed for instance as the spins (equal angles) directions of electrons in an atoms shell. For the dihedral D_6 with characteristic polynomial $z^6 - 1$ it sets many numerical or (quasi-)particle cycles: six color charges, six electrical charges, six energies, six mass weights for fermionic series. As model exists the G-compass (figure 1) where the 2x2-matrix G of order 6 has the first row (1 -1) and second row (1 0). It belongs to the normed general relativistic scaling factor of Minkowski to Schwarzschild metric.

The coordinate complex multiplication in C^4 is necessary for the functional computations in physics spacetime. The four real coordinates (x, y, c, t) are complex extended. In the octonian interpretation, the doubling of coordinates is different from the earlier complex/quaternionic (z_1, z_2) spacetime coordinates. Take for octonians (e_0, e_1, \dots, e_7) and match $(e_1 = x, e_5 = m)$ and $(e_4 = t, e_6 = f)$ according to the two Heisenberg uncertainties position-momentum and time-energy (as $E = hf$). To a polar angle is added $(e_2 = \varphi, e_7 = \exp(i\varphi))$ (e_7 is linear but projective stereographic closed to exp) for EMI and $(e_3 = \theta, e_0)$ is for a spherical angle θ and the compass vectorial needle e_0 . Beside linear xyz-space Euclidean coordinates are then spherical coordinates (r, φ, θ) available in space R^3

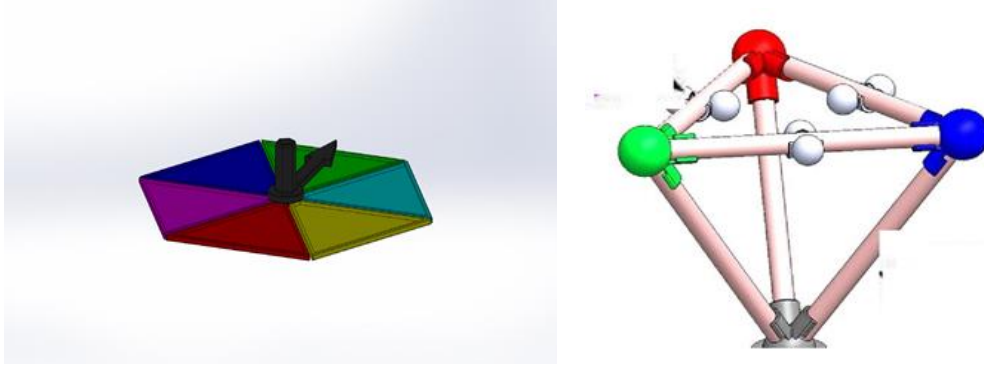


Figure 1 G-compass, nucleon tetrahedron at right with the tip of a rgb-graviton at the bottom and the quark triangle on top

2. Other matrix multiplications and systems

Octonians have a different multiplication table than the GellMann matrices λ of SU (3). The gluons dimension is also 8 and signed SU (2) generators 8 dimensions have the quaternionic multiplication.

The vectorial space SU (2) extension is (z_1, z_2, z_3, z_4) . As C4 it has the complex multiplication.

To the former spaces 1234 (WI/EM), 3456 (GR/SI), 1256 (EMI) is added another GR space 07 for the three linear dependent σ_3 matrices. The three $\lambda_{8,9,10}$ complex coordinates use for their location the symmetry of the third roots of unity as solutions of the characteristic equation $z^3 - 1$ of a difference equation with three Fibonacci like sequence solutions $1 = 1n, p1n$ (equal to $1, p1, p2$), $p2n$ (equal to $1, p1, p2$). The flat compass three 120 degree turns of e_0 set barycentric coordinates for the $(1, p1, p2)$ triangle. The Higgs field or boson can sit at their intersection B as barycenter a mass for matter systems. At least 3 dimensions are needed for such systems. Color charges in superposition of (red-green-blue) conic rgb-gravitons whirls set a spin-like GF base triple and the mass of a nucleons three quarks sit at the end of the base vectors and are located on the former flat triangle vertices. As a measuring apparatus, a superposition second GF has the above rescaling of the nucleons mass. At red can sit the sum of the quark masses as new vector, at blue the frequency transformed mass and at green some interaction energy transformed mass. The GF adds these masses for the nucleons mass, set at B. The GF act through a change of states, described in [1] as a SI rotor, having for its symmetry the D3 dihedrals group of order 6 (see also the next section).

The SI rotor is for integrations of functions. The location of differentials for this in tangent spaces is described by the coordinates, r and dr , x (y or z) and dx (dy or dz), t and dt or Δt as interval. Sometimes speeds v (or ω) are used as variable and dv appears for instance in $dv/dt = d^2v/dt^2$ as kinetic force acceleration. Angular derivatives $d\phi$, $d\theta$ appear in the two Einstein metrics.

For differentiation or quotients the Heisenberg pairing of octonian coordinates 15 sets for x on 1 the functional derivate d/dx on 5, for 46 on 4 time and $6f = 1/\Delta t$ or as d/dt , complex differentiation d/dz is on 12 as complex plane. Complex contour integration dz is on 07 for complex functions. In the real case also locations for area dA and volume dV integrations and differentiations are set. For manyvalued functions, differential equations are used for getting solutions of problems. The difference equations, used above for rgb-gravitons, can be extended for Fibonacci like sequence solutions in other cases. The sequence $(-1)^n$ with solutions $+1, 1$ as unit sphere S_0 and characteristic polynomial $z^2 - 1$ sets for circular rotations a mpo counterclockwise or cw clockwise orientation. The characteristic polynomial $z^4 - 1$ has in as sequence with solutions $1, i, -1, -i$ for weak bosons $W+, W-, Z_0$ and a hyperphoton, $z^6 - 1$ is for the G-compass solutions (6th roots of unity for electrical charges, 6 color charges, 6 energies, a complex kg-mass GF for leptonic series). Th G matrix has as eigenvector $(-p2, 1)$ with eigenvalue $-p1$, the first sixth root of unity. It presents an observable state of a measurable system like the G-compass and describes with its powers the sixth roots of unity possible positions of the G-compass needle.

The use of dihedrals D_n with symmetries of order $2n$ is extending the discrete version with characteristic polynomials for differential or difference equation solutions. The setting of n poles on a circle is for complex functions and charges. They can be used as sources or sinks which can also be identical as for closed magnetic field lines. Heegard decompositions of unit spheres show the solutions surface geometries in this case. Splitting a circle at one point as pole gives an interval with two poles at its ends. Potential field lines are set about the poles. For two poles on D_2 the circle

split into two intervals I_j . When the endpoints of I_j are identified, a real projective line is obtained with one stereographic point ∞ for the circles projection onto the tangent of the circle at the diametrical opposite point on the circle. Stereographic maps occur in any dimension of a unit sphere S_n and are used by gravity. For two vectorial oriented vectors as $I_1, 2$ the spin up/down directions are mentioned.

If the dimension is increased, the S^2 is Heegard decomposed at an equator into two hemispheres. As projective closures arise two projective planes P_j^2 . They occur in the MINT-Wigris model as an atmosphere about a nucleon or atomic kernel where this system exchanges its energies with the environment along an x-, y- or z-axis, orthogonal to the chosen equator (figure 2, [1])

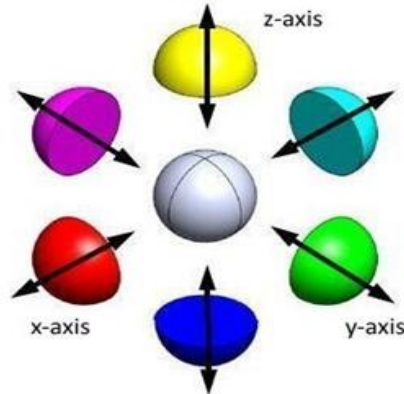


Figure 2 hedgehog for deuteron with color charge P^2 polar caps and vectors, turning up or down like spin on a P^2 Moebius strip for the energy exchange out/in direction

In 3 dimensions, the polar structure on D_n allows a decomposition of the Hopf sphere S^3 into brezels of genus 0, 1, 2... The torus (genus 1) is for leptons, genus 2 is for quarks, genus 3 for nucleons...

For the torus there are 3 geometrical versions, the usual surface with a horizontal core inside the torus and a rotation axis through the center of its horizontal diameter d with. In a vertical transversal section figure 4 shows first the electrical charges torus as two disjoint circles. In the figure below the two circles distance d' is contracted to 0 and a singularity of the torus on the axis is obtained for a dark matter Horn torus, when the two circles overlap (last part at left) a spindle torus arises for neutral leptons geometry. When a vertical circle is retracted to a point, a pinched torus is obtained for dark whirls. The core is not a carrier for mass.

The examples below show that the complex functions poles have for particles and nucleons different geometrical shapes of surfaces available where the energy is stored inside. The functions arise as solutions of differential equations. The energies of inner spaces having these boundaries have another dynamics than the observable equipotential or field lines about complex poles show for functions.

Concerning subspaces of octonians, some additional remarks are:

In a unification of gravity E (pot) and electrical EM (pot) potentials, three 4-dimensional spaces are obtained as projections from a common 5-dimensional field [6]. In the authors theory they are

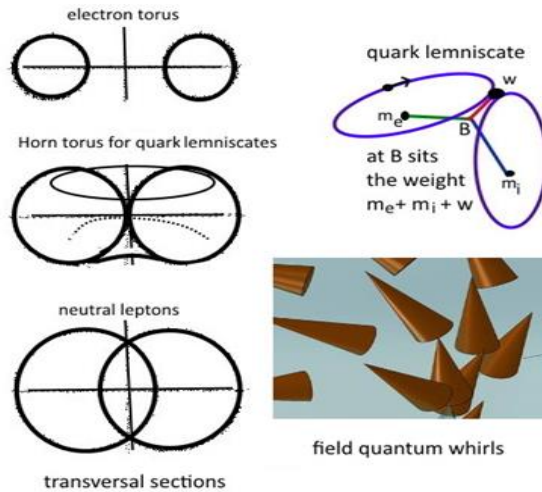


Figure 3 transversal sections through tori at left, a quark lemniscate with two poles at upper right, below conic magnetic field quantum whirls

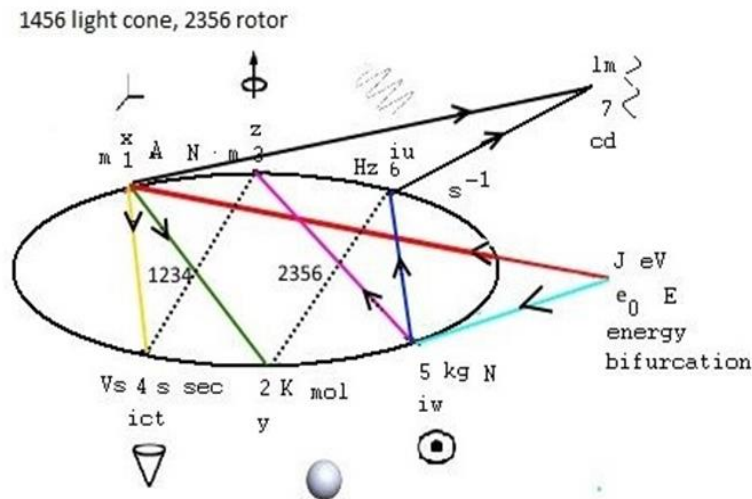


Figure 4 Pascal bifurcation for octonian coordinates, listed by their indices; three 4-dimensional spaces 1234 (spacetime, EM+WI), 1456 (EMI), 2356 (GR+SI) are obtained by projective projections; logos are added which relate to the coordinates use: spin GF quasiparticle triples at 1.

heat volume bubbles for phonons at 2; at 3 a rotation axis perpendicular to a plane for a systems orbit, rotating about a barycenter; at 4 conic whirls for magnetic field quantum; 5 barycenter in a disk or volume; 6 helix line or its cosine projection for frequencies, also for 7; the associated energies measuring unities are added as quality renamed from the above 1234, 3456, 1256 with other octonian indices replacing the coordinates where 1234 is for spacetime, the electrical potential and the weak interaction, 1456 is for EMI as a neutral (scalar) field and 2356 is for gravity and the strong interactions potentials. In an energy Feigenbaum bifurcation (figure 4) the three spaces occur on the Pascal line as points in which two intervals of the Pascal figure intersect. The bifurcation is from e_0 , drawn at left as a vector, to E (pot) 5, EM (pot) 1. EM (pot) bifurcates (the Pascal intervals are drawn) into E (magn) 4 and E (heat) 2. E (pot) bifurcates into E (kin) 6 and E (rot) 3, kinetic and rotational energy and as output is drawn EMI 7, generated by 1,6 (wave length λ 1 and frequency f 6 in $\lambda f = v$, v speed). In figure 5 the octonian diagram shows the Pauli σ_j , $j = 1,2,3$, GF as lines 123, 145, 167, 246, 257, 347,356 generation in the Fano memo. There are similar GF's, arising from the GellMann SU (3) matrices.

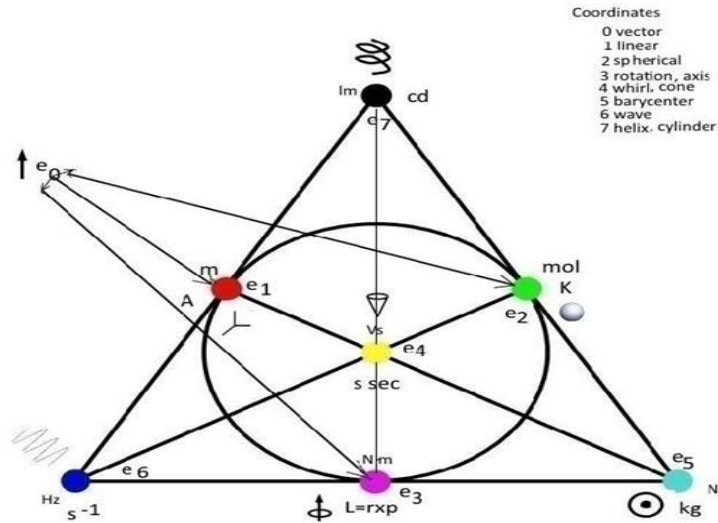


Figure 5 excluded is e_0 at left; the intervals are 3-dimensional spaces with the three base vectors drawn as points on the interval; projective, any two 3-spaces have a line in common; 123 as circle drawn is xyz-space; 145 is EM with charge, magnetic momentum and induction (also used for neutral leptons with momentum replacing magnetic momentum); 167 is EMI; 246 is heat; 257 is for barycenters with a mass scalar, 347 is for rotations; 356 is for the strong interactions SI rotor (see [1])

3. Quantization and States

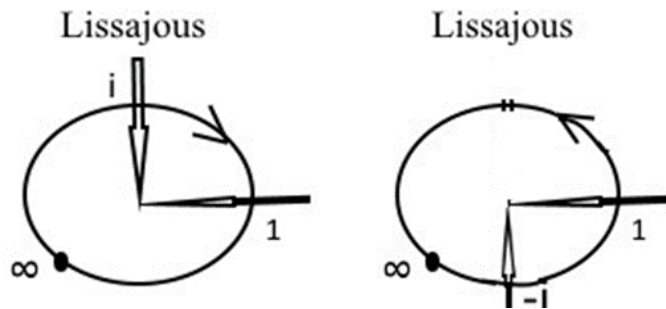


Figure 6 Lissajous for two orthogonal hitting frequencies f_j in proportion 1:1; an amplitude length r of the incoming frequencies is taken as radius of the circle

In figure 6 is drawn a model for two hitting frequencies. It is assumed that the circle is not at rest, but rotating in the described way. The time reversal operator T can stop. This means for the CPT Klein group $Z_2 \times Z_2$ that it is factored by Z_2 to the group $\{id, P\}$, P parity. The energy on the circle is then at rest and it can be assumed that through $mc^2 = hf$ the frequency $\omega = 2\pi f$ is transformed into a mass scalar where the circle carries as weight in kg the energy. This means that P as point reflection or rotating angle of 180 degrees factors the geometry of the circle by identifying diametrical opposite points. There is no orientation on the obtained real projective line P^1 with coordinates $[x,w]$. To the circle is added in this coordinate description a point at infinity ∞ which can be $[1,0]$ or $[0,1]$ and the stereographic map projects from this point the circle down to the circles tangent line g at the diametrical opposite point B to ∞ . A metrical distance dr or r , radius, is set on g by choosing a unit vector where the vectorial compass needle e_0 from B to its units endpoint has no orientation.

The reverse situation, when such a circle splits into two frequencies means that the circle is decomposed into two cosine, sinus wave intervals, having equal amplitudes, through cutting it at the points B, ∞ . This kind of decomposition is available in higher dimensions, known by the Heegard decompositions of the Hopf unit sphere S^3 into two solid balls or two brezels of genus $n = 1, 2, \dots$

In 2 dimensions, the complex line, drawn as unit sphere S^2 splits at an equator A. In this case the three xy, xz, yz planes can serve for the decomposition.

Instead of two cosine, sinus waves with an amplitude, two hemispheres as polar caps u, c(u) of the hedgehog arise. c(u) is the anticolor of u and the charge u or c(u) at rest means that the polar cap carries this charge like a condenser plate on its area. For the three planes red-turquoise for u is along the x-axis, green-magenta on the y-axis and yellow-blue on the z-axis (figure 2). The curved shape of the hemisphere can be interpreted as a wave-like membran oscillation. The hemisphere in motion can swing up-down through a horizontal disk with the boundary A. This is more like an action of the quasiparticles solitons (figure 7) which change with their amplitude density as matter per volume by changing the metrical area measure πr^2 of the disk. For the amplitude can be taken the metrical, angular length πr of the hemicircle, stretched from the linear Euclidean measured diameter $2r$ to about $r \cdot (3.14)$.

Adding speed means that the Z2 group of parity P is extended by the time reversal operator T and includes their product $PT = C$ as conjugation operator with symmetry $Z2 \times Z2$. For the 1-dimensional case of a mass carrying circle P1 at rest the extended group adds the two orientations clockwise cw or counterclockwise mpo in figure 6 with signed speeds -v or +v. Orientations are computed through the sign of a matrix determinant. In this case, the first row of this matrix is (1 i) for a space vector i. For the second row the base vector of the xy-plane is chosen from which the rotation starts, (1 0) or (0 i). The determinant is then -i or +i. Set in motion, its energy as frequency ω is replacing mass at rest. Only full windings $n = 1, 2, \dots$ about the circle A count it as energy discrete $E = hf$. Complex variables count windings about A through contour integration $n = (1/2\pi i) \int_A dz/z$ as one of the variation values of the integrated complex $\log(z)$ function as inverse function to exp with $\exp(it + 2i\pi n) = \exp(it)$. The physics notation is $T = 1/n$ for the circulation time as period and for the orbital speed on A with frequency $f = n$ holds $\omega = r2\pi n$, r radius of A.

This accounts for the spin length quantization of energy $E = hf$. Energy levels of systems are quantized

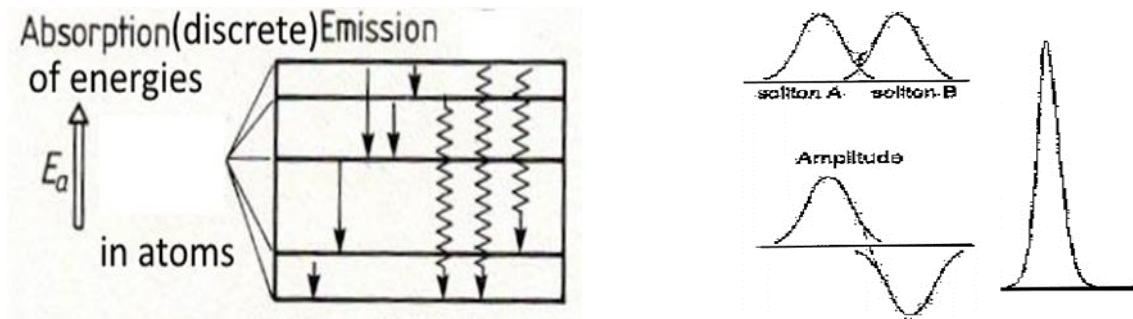


Figure 7 energy levels at left, soliton at right

The basic Planck number spin length are normed to $\frac{1}{2}$ for fermions, 1 for bosons and 2 for gravitons, which is another length expansion/contraction as mentioned above for the membran oscillation. A physical explanation exists for these spin values. In the MINT-Wigris research the rgb-graviton whirls action is quoted for this. Beside the stereographic map, introduced above, they use an orthogonal, spiralic projection map. If transversal sections through a whirl are drawn as in figure 8 at right, the whirl rotation changes the (accoustic drawn) position of a triangle as in figure 8 at left. The proportions on spiralic rays for the rgb-graviton orthogonal (middle part figure 9) contraction/expansion on the whirl are $\frac{1}{2}:1:2$. The values arise through permuting three reference points 0,1, ∞ on the Lissajous circle in figure 6. The point 0 is in this notation diametrical opposite to ∞ and 1 is in projection the length of an octonian compass e0 needles endpoint. The circle is expanded to a complex Riemannian, real 2-dimensional sphere S^2 with these points on an equatorial circle. The complex cross product allows six (cross ratio) Moebius transformations when z as fourth member is added, $z, 1/z, 1-z, 1/(1-z), z/(1-z), (1-z)/z$ for the permuted reference points. Setting as initial value the rgb-graviton spin length $z = 2 = |z/(1-z)|$, a degenerate numerical orbit is obtained by $1/z = \frac{1}{2} = |(1-z)/z|, |1-z| = |-1| = 1 = |1/(1-z)|$. The six permutations present the dihedral D3 symmetry of a nucleons quark triangle

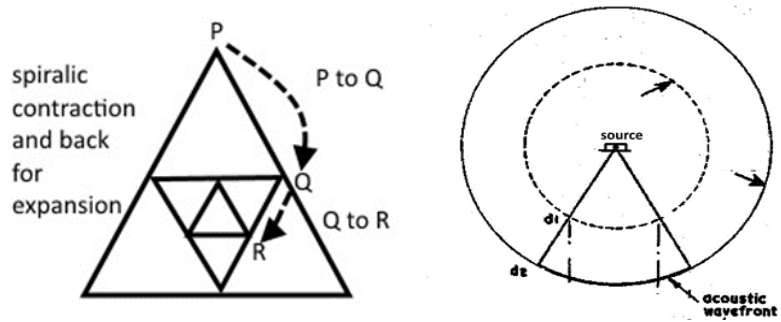


Figure 8 nucleons quarks triangle contraction/expansion at left, acoustic wave front with a spiralic expansion at right

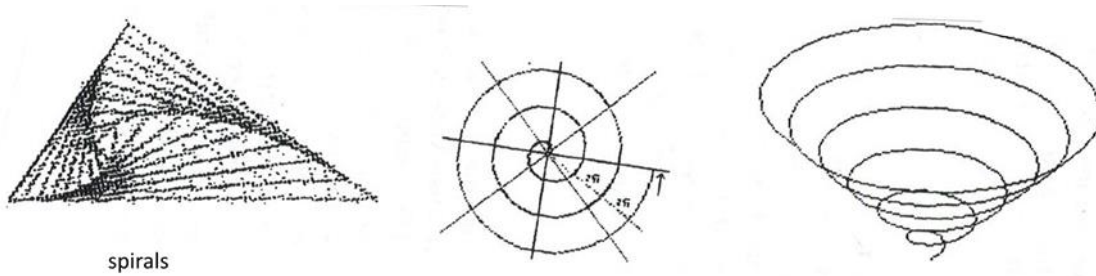


Figure 9 two 3-dimensional spirals at left, right, middle flat spiral as observed for two hitting galaxies (with a common barycenter) orbits

In the MINT-Wigris research another representation is used for the strong interactions SI rotor. It describes the extended gluon exchange between quarks where the rgb-graviton is used for the tip of the tetrahedron as in figure1. Several videos are available for the dynamics and figure 10 shows a model for it. Single axes are set and a conic rotation cw or mpo is alternatively made about the changed axes in a cycle. The six half cones as membrans join to three cones and a cosine-like amplitude oscillation occurs on the cones three bounding circles orthogonal to the triangles plane.

Keeping either r red or g green fixed for rotating the other two color charge vectors presents the six permutations of rgb as rgb, brg, grb, gbr, bgr.

The SI rotor sets barycentric coordinates in the quark triangle as the three axes in 120 degree angles to one another. At their intersection as barycenter, a Higgs field or boson sets the rescaled mass of the nucleon (see also the former section).

The SI rotor describes an inner dynamics for nucleon CP^2 space. A matter wave presentation for a nucleon is no included in this model. This is on particle and interaction base and a wave description

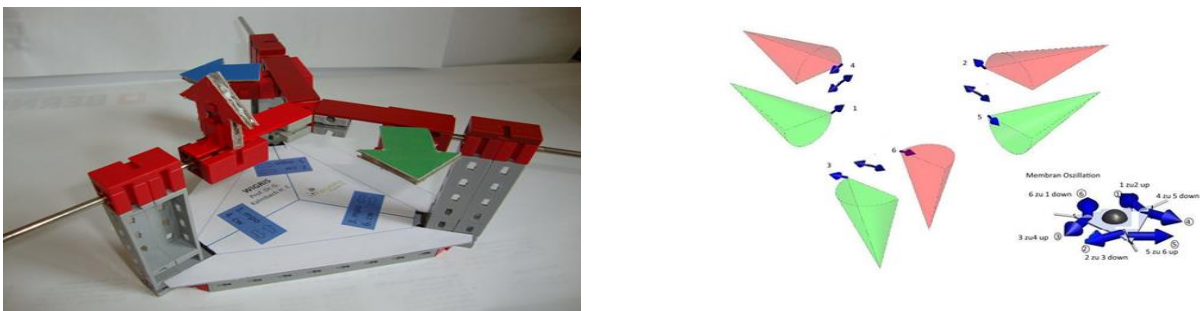


Figure 10 SI rotor at left, six states as half cones (membrans) at right, – lower part right - the blue momentum vector fixes the quark barycenters at the triangles vertices

needs other sources. For the solition of a Schroedinger equation the rescaling of nucleons mass would mean that as a wave package it generates a group speed equal to a relativistic speed with which the sum of the quarks masses is rescaled. In section 2 a spin-like kg measuring GF was described for this which belongs to an rgb-graviton. Its three base vectors are named red, green, blue, but in this version the color charges nor the rgb-graviton are not carrying mass. If the three color charge whirls are drawn as vectors, not as whirls, they present $E(\text{pot})$ as red force, $E(\text{rot})$ as green force and $E(\text{kin})$ as blue force. All three have a kg measured mass scalar in their definition and the postulated superposition kg GF of rgb-gravitons is drawn as three vectors attached to the quarks barycenter as vertex of the nucleon triangle. The center of the kg-mass GF is replaced by the circumference of the triangle on which the three vectors initial points sit. The video for the SI rotor shows the six states for their 3-dimensional positions. The first state is in figure 10 left. Other states are.

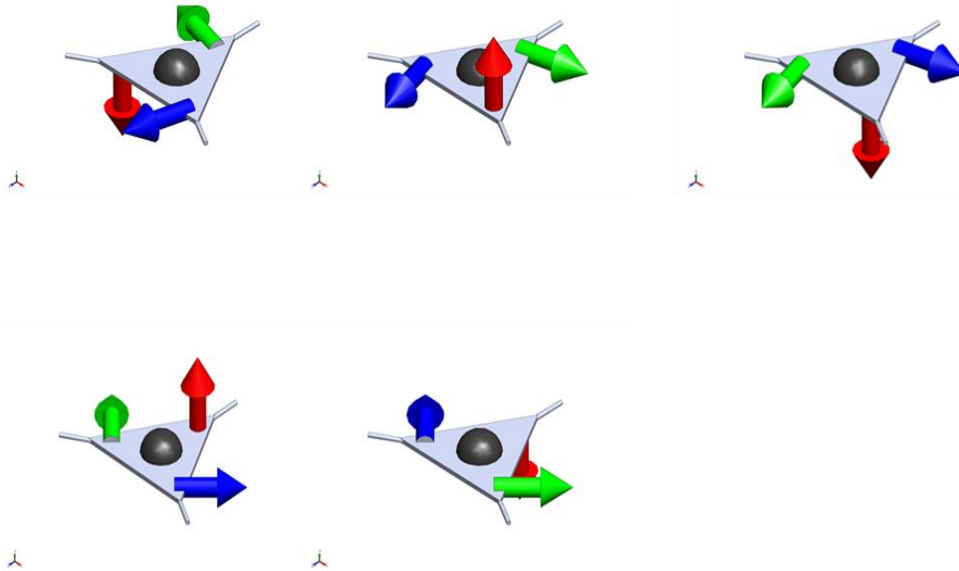


Figure 11 SI rotor dynamics with the first state at left in figure 10

4. Hilbert subspaces

In section 1 the new tools G-compass for octonian e_0, e_7 coordinates and the nucleon tetrahedron with an rgb-graviton whirl added to a nucleons quark triangle show how new spaces, dihedrals, measuring apparati like the GF, projective spaces can serve for a unified theory which includes gravity.

The 4-dimensional Hilbert space H_4 model for spacetime has usually the Euclidean metric, which is only kept for space. Adding time needs according to Einstein the affine Minkowski metric which keeps the area of length with time constant, $l \cdot t = l' \cdot t'$ when two coordinate systems are in special relativistic motion against one another. General relativity adds projectivity to this and a nonlinear rescaling of this metric where for the differentials the area is preserved $dr \cdot dt = dr' \cdot dt'$, r radius. The projection operators of H_4 generate on closed subspace decompositions similar graphs as the Fano memo where a subspace lattice structure L is listed by an interval containing 3 or 4 points. Blocks as maximal Boolean subspaces can overlap in their 4 base vectorial lines in one or two subspaces. The overlapping graph in form of a nucleon triangle means that quarks color charges are extended to a block for rgb-graviton whirls such that their tensorial $\cos(\omega(t-z))$ waves can use time. The lattice structure of L requires flashes (figure 12). The octonian spacetime coordinates 1234 are at the ends of the four blocks, for octonians doubling of coordinates 1 extends by splitting in H_4 its vector $1x$ into two vectors $1x, 5f$ for the first Heisenberg uncertainty, 2φ into $2\varphi, 7\exp(i\varphi)$, 3θ into $3\theta, 0e_0$. This block diagram is used often in the L graph, whenever a 4-cycle occurs where the outer adjacent pairs of the astorid as $uv = 12, 23, 34, 14$ are extended to blocks uvw with different base vectorial lines w, p of H_4 drawn as $u \circ - \circ w - \circ p - \circ v$. The mathematical proof has the octonian and the existence of rgb-gravitons whirls as an interpretation [9]. The author refers to the accepted view in physics that the Einstein energy-momentum tensor computation is interpreted as spacetime ripples which they attribute to graviton waves. This geometrical interpretation has also other interpretations [1]. Added is in this article that the solitons amplitude change for density per volume can be included for changing metrically the matter volumes radius r where the matter is kept at rest. For mass of matter is quoted that also in the inversion to dark matter

the Schwarzschild radius R_s inversion sets the dark matter radius r' to $r' = R_s^2$ with reducing projective 3-dimensional quarks to their 1-dimensional lemniscate core in figure 3 at upper right. Mass is at rest and not rescaled. The 1-dimensional circle S^1 cores for mass in R_s are present in the Hopf S^3 and the atomic kernels S^5 fiber bundles which use it also as fiber and EMI uses it as symmetry and Kaluza-Klein $U(1)$ projective closed octonian e_7 line.

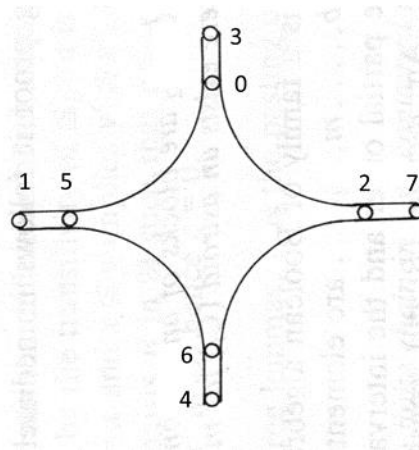


Figure 12 the curved intervals present blocks as 4-dimensional spaces having a four vectorial base in H_4 , numbered with octonian base vector indices $0,1,\dots,7$; the adjacent blocks have

2-dimensional subspaces in common, in the Fano memo only 1-dimensional subspaces; this is not a 8-dimensional block, but instead the four 4-dimensional blocks get a functional exp interpretation

In section 1 the cross product extensions, real or complex, show that not only one physics 1234 block is important, but in its different cross product extensions other 2356 SI, 1456 EMI and projective 123456 normed R_5 (see [6]) spaces, projective planes $[u,v,w]$ for the hedgehog caps and quasiparticles GF's as 3-dimensional orthogonal bases occur. For unit spheres S_n dimensions in these spaces not only the fiber bundles and $U(1)$ are important, but also $S_0 = \{+1,-1\}$ as Boolean block logic $\{0,1\}$ true, false which fails for L . Hilbert space also in infinite dimensions has no valid Boolean implication, modus ponens, deduction theorem. Paradoxies as listed in the internet are not revised by Physics logicians ☺ which disregard these L facts, proved in [9]. L has a very weak implication, for H_4 the projective modular law (any two lines have a point in common, no parallels exist, Einstein still allows them for the affine Minkowski metric) which is weaker than Boolean modus ponens. Boolean reasoning for subspace structures is only allowed in blocks, not in L .

Deductions [from laughing to [9] ☺ in the internet] are neither allowed for L and quantum structures.

In section 2 some new results for the weak interaction are included. Examples for GF's are the electromagnetic induction as angular momentum, arising for a loop current and a magnetic field, crossing the loops areas, for neutral angular momentum it is the equation $L = r \times p$, p momentum.

The early development of the universes energies is postulated before Planck time as a bifurcation. From a dark matter explosion, listed as the octonian e_0 compass vector with its huge common EM+GR potential field of [6] added the two EM 1 and GR 5 octonian EM charge and mass vectors bifurcate with added fields 1234 and 1256. Then 1 bifurcates into 24, sets the GF 145 for EM and 246 for heat. 5 bifurcates into 36, sets 347 for rotational energy and 167 for kinetic energy after the final bifurcation from 16 to 7 with the EMI GF 167 occurs which happens much later than where Planck numbers are generated and physical laws can be applied. For speed of light c as a basic Planck/Einstein natural constant a similar inversion as for the dark matter R_s radius inversion occurs. The mathematical inversion at a circle, as Moebius transforamtion $z \rightarrow 1/z$ allows for dark energy speed v' inversions at the Minkowski cone line $v = c$ as $v'v = c^2$ for speeds $v' > c$ inside a pinched torus (last model in figure 13 which is also for dark accoustic sound whirls in the universe).

For the matter speeds $v < c$ in the universe is in [7] also blamed Minkowski special relativistic rescalings. For a Schroedinger wave package solution, the wave momentums optical computed speed $v = \partial\omega/\partial k$ has to be computed special relativistic as a mass rescaling with an additional differentiation according to speed ∂v . It is also responsible for inertial mass where mass as force is integrated to potential for setting a resistance to be removed from ist momentums speed. Planck found the second constant h for the Planck time in Einstein's $E = hf$, R_s sets the gravitational constant and

heat recals E by Kelvin k as constant. The EM constants are set e as electrical charge when weak bosons W+, W- and their decay leptons are generated and $\Phi_0 = h/2e$ as magnetic field quanta energy is set, EMI measured is cd candela, set later on in the development of the universe when photons can escape from atoms in spectral series and the dark universe gets light.

In section 3 the Lissajous figures show how the EMI helix f and leptonic angular $\omega = 2\pi f$ frequencies generate the U(1) and fiber circles, having no orientation and as projective P1 get a stereographic point ∞ added for GR projection operators stn, used in any dimension Sn. The complex line as S^2 adds the cross ratios the diametrical opposite point 0 use for the origin in the tangent plane at 0 to S^2 and in between a mpo rotational point 1, projected into the xy-tangent plane as an octonian unit vector e0. It sets for all energies the GF units as meter, Ampere, kg, k Kelvin, Φ_0 Tesla, second/time, cd EMI and for itself it sets the six color charges in the G-compass by turning in the 6th roots of unity directions (figure 1) where the color charge has a condenser plate one segment. If the G-compass decays into 6 segments, their two bounding radii are identified to form a conic color charge whirl, they can be in superpositions of 2, 3, and 6.

In section 3 quantizations and geometrical dynamics presenting finite sets of states are demonstrated with models. To the flash model (figure 12) is added the functional interpretation where the block 4627 and 1546 are for Ψ EMI waves and particle Ψ matter waves while 0327 has the $\exp(i\varphi)$ or $\exp(-i\varphi)$ functions in complex variables form $\cos(\varphi) + i\sin(\varphi)$ or $\cos(\varphi) - i\sin(\varphi)$. In more detail, the extra Ψ values are projective 5-dimensional extensions of the 4D-blocks; EMI waves have as exp function the scaled variables t,x and constants angular speed ω (as 6) for energy E multiplied with time t (as 4) and the wave number (inverse scaled circular wave length λ as 7) k multiplied with +y or -y (as 2) for the space direction of its world line. In the Schroedinger matter wave solution 1546, ω is replaced by energy $E = hf$ as 6 and k by the momentum p with $\lambda p = h$ as 5, the world line is on x as 1. The sign of it is according to the exp wave taken on a circle for clockwise cw as - and counterclockwise mpo as +. 0327 has $\exp(i\varphi)$ or $\exp(-i\varphi)$ functions with this interpretation of sign as 7; 0 is for a radius and polar complex coordinates as 07; 2 is for a measured angle φ towards the radius direction and as 3 normal or 3-dimensional, scewed towards the 07 plane, is an observable rotation axis or a as vector, leaning in a θ towards the space z-coordinate, for a conic rotation with axis z; the spherical (r,φ,θ)

3-dimensional 032 space is extended by 7 for cylindrical U (1) coordinates. In 1503, as 5 acts quantized frequency $f = n$, an integer valued winding number in a time interval $\Delta t = 1/n$, also signed in + cw rotational or - form by applying the time reversal operator; f can use $f = mc^2/h$; angular speed $\omega = d\varphi/dt$ is on 3, 02 are polar plane coordinates (r,φ) . Winding numbers are computed by complex contour integrations (with residue $1/z$ for instance) about a simple closed curve, like a circle; this quantizes energy $E = hf$ and spin lengths.

Whirls (in 0327 or 1503, figure 8,9) are a third energy character 3, added to the physics particle-wave energy character of 5 or 7, bound to mass/barycenters 5 and EMI 7. A GF 357 can be used (figure 13). The use of accoutic heat related whirls is accepted in physics. The quasiparticles are phonons

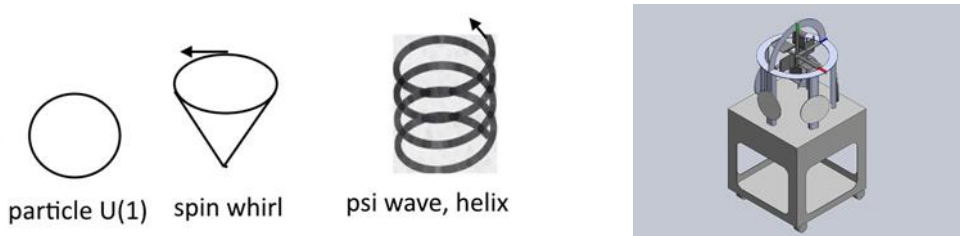


Figure 13 three energy characters, particles with the first figure have also a barycenter of the circle added, computed by setting barycentric coordinates; for them also the lever law is available and the wheel at right

As last figure of models is added a survey for the MINT Wigris Tool bag. It can be GF extended by about 20 more such constructions in future. They need more research to be done, especially for quasiparticles.

Figure 14 Tool bag, some models are shown earlier, the 6 roll mill and gluon exchange belong to the SI rotor as crystal or flow, deuteron shows projection maps of a deuteron boundary S^2 onto a tangent xy-plane where the projected S^2 radius is changing length when the xy-plane is parallel moved to a plane A, the template (handycrafts) can be extended for drawing easily on paper with pencil other figures, cut out and rolled for instance for the geometry of periodic functions on cylinders, torus or Moebius strip figures; the models for the dark range show a Horn torus with a singularity in the middle for dark matter and a combined dark/whirl, dark energy pinched torus where the helix EMI coil has to be

removed for dark acoustic whirls. - the Minkowski cone is in this case closed at projective infinity by a circle whils in the cylindrical EMI case the cylinder is closed by one point at infinity: for photons the leptonic torus has one transversal circle be retracted to a point where an electron for instance releases part of its ω frequency and changes its state between two Bohr radii; since attached spin energy is quantized, the main quantum numbers n occur and are used for transforming with the use of the Rydberg/Feinstruktur constant the ω frequency into the EMI cd frequency; it has as geometry for a photon one helix winding on an EMI cylinder which can be linearly drawn with drawing on paper two lines, cut out and glued together by the template; the models and the Tool bag have DPMA patents and can be bought for MINT education courses in Germany. In figure 13, the wheel is a tool, showing three Euler angles rotation which generate the single x, y, z space coordinates for the tetrahedron GF in figure 1. In figure 10 the single barycentric coordinates are generated by the SI rotor. Another model can be constructed for the 4-dimensional case of spacetime, presented in figure 12 or as a condensor plate as the quadrangle for the magnetic group. If two such plates are set parallel with the spacetime coordinates as diagonals, a rotation by a 45 or 135 degree shows in central projection a dihedrals 8-edge for presenting geometrically the generated s octonians. In [5] for deuteron such a model is shown in the 3-dimensional case where a proton and neutron tetrahedron ar joined at their rgb-graviton tips and the quark triangle show in central projection a dihedral 6-edge

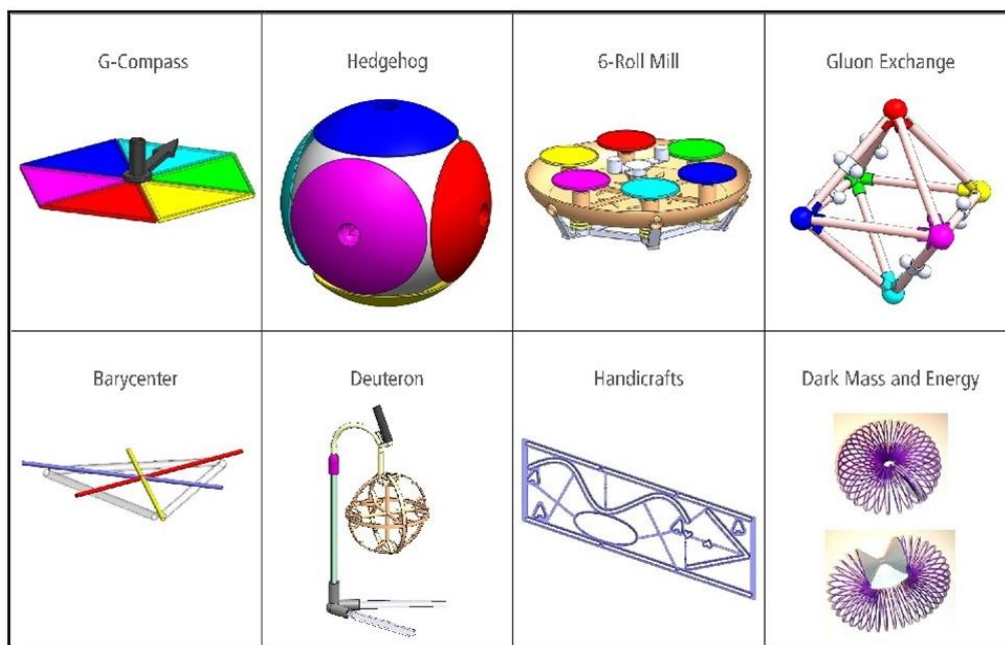


Figure 14 the Tool bag with 8 models

5. Conclusion

Space presentations is one theme of this investigation, Hilbert space blocks in 4 dimensions are important, in 3 dimensions the GF measures based on real cross products are setting the quantum mechanical measuring process. Interactions are unified, models for them are constructed.

References

- [1] G Kalmbach HE. MINT-WIGRIS, MINT Verlag, Bad Woerishofen. 2017.
- [2] G Kalmbach HE. (Chef-Hrsg), MINT (Mathematik, Informatik, Naturwissenschaften, Technik), MINT Verlag, Bad Woerishofen. 1997-2020; 1-65.
- [3] Internet video under YouTube: Moebius Transformations Revealed. 2014.
- [4] G Kalmbach, U Eberspaecher. MINT-Wigris Tool Bag, Bad Woerishofen. 2019.
- [5] G Kalmbach. MINT-Wigris Postulates, in: researchgate.net under MINT-Wigris Project. 2020.
- [6] E Schmutzer, Projektive einheitliche Feldtheorie, Harry Deutsch, Frankfurt. 2004.

- [7] K Stierstadt. Physik der Materie, VCH, Weinheim. 1989.
- [8] MINT-Wigris project (G. Kalmbach H.E.), in the internet under: [researchgate.net](#).
- [9] Kalmbach G. Orthomodular Lattices. – London New York: Academic Press. 1983; 390.